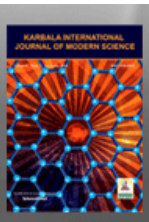

Karbala International Journal of Modern Science

Volume 8 | Issue 3 Article 24

Molecular Docking and Dynamics Simulation Studies to Predict Multiple Medicinal Plants' Bioactive Compounds Interaction and Its Behavior on the Surface of DENV-2 E Protein

Arief Hidayatullah
Department of Biology, Faculty of Mathematics and Natural Sciences, Universitas Negeri Malang, East Java, Indonesia

Wira Eka Putra
Department of Biology, Faculty of Mathematics and Natural Sciences, Universitas Negeri Malang, East Java, Indonesia; Department of Biotechnology, Faculty of Mathematics and Natural Sciences, Universitas Negeri Malang, East Java, Indonesia, wira.putra.fmipa@um.ac.id

Muhaimin Rifa'i
Department of Biology, Faculty of Mathematics and Natural Sciences, Brawijaya University, East Java, Indonesia

Sustiprijatno Sustiprijatno
Indonesian Center for Agricultural Biotechnology and Genetic Resources Research and Development, West Java, Indonesia

Diana Widiastuti
Department of Chemistry, Faculty of Mathematics and Natural Science, Universitas Pakuan, West Java, Indonesia

See next page for additional authors

Recommended Citation

Hidayatullah, Arief; Putra, Wira Eka; Rifa'i, Muhaimin; Sustiprijatno, Sustiprijatno; Widiastuti, Diana; Heikal, Muhammad Fikri; Susanto, Hendra; Salma, Wa Ode; and Mulyadi, Hilal (2022) "Molecular Docking and Dynamics Simulation Studies to Predict Multiple Medicinal Plants' Bioactive Compounds Interaction and Its Behavior on the Surface of DENV-2 E Protein," *Karbala International Journal of Modern Science*: Vol. 8 : Iss. 3 , Article 24.
Available at: https://doi.org/10.33640/2405-609X.3237

Molecular Docking and Dynamics Simulation Studies to Predict Multiple Medicinal Plants' Bioactive Compounds Interaction and Its Behavior on the Surface of DENV-2 E Protein

Abstract

The envelope protein (E) is a fusion class II protein that is essential for DENV fusion. We use two active compounds derived from commonly used plants in Indonesia: galangin and kaempferide. We ran a docking and 1000 ps molecular dynamic analysis with normal physiological parameters. During the simulation, galangin and kaempferide binding sites fluctuated. But chloroquine has lesser ligand mobility, hence keeping contact with fusion loops, whereas both drugs lose contact with hydrophobic pockets. However, the two active compounds have a more stable ligand configuration. Less than 2 Å alterations were seen in the RMSF simulation of the protein E residues. In a 1000 ps simulation, all tested compounds form stable complex with protein E, demonstrating that the two active compounds may be predicted as DENV-2 E protein fusion inhibitors, despite chloroquine inhibiting in a unique manner linked to its interaction domains.

Keywords

Anti-viral; DENV-2 E protein; Molecular dynamic; RMSF.

Authors

Arief Hidayatullah, Wira Eka Putra, Muhaimin Rifa'i, Sustiprijatno Sustiprijatno, Diana Widiastuti, Muhammad Fikri Heikal, Hendra Susanto, Wa Ode Salma, and Hilal Mulyadi

RESEARCH PAPER

Molecular Docking and Dynamics Simulation Studies to Predict Multiple Medicinal Plants' Bioactive Compounds Interaction and Its Behavior on the Surface of DENV-2 E Protein

Arief Hidayatullah [a], Wira Eka Putra [a,b,*], Muhaimin Rifa'i [c], Sustiprijatno [d], Diana Widiastuti [e], Muhammad Fikri Heikal [a], Hendra Susanto [a,b], Wa Ode Salma [f], Hilal Mulyadi [b]

[a] Department of Biology, Faculty of Mathematics and Natural Sciences, Universitas Negeri Malang, East Java, Indonesia
[b] Department of Biotechnology, Faculty of Mathematics and Natural Sciences, Universitas Negeri Malang, East Java, Indonesia
[c] Department of Biology, Faculty of Mathematics and Natural Sciences, Brawijaya University, East Java, Indonesia
[d] Indonesian Center for Agricultural Biotechnology and Genetic Resources Research and Development, West Java, Indonesia
[e] Department of Chemistry, Faculty of Mathematics and Natural Science, Universitas Pakuan, West Java, Indonesia
[f] Department of Nutrition, Faculty of Public Health, Halu Oleo University, Indonesia

Abstract

The envelope protein (E) is a required fusion class II protein for DENV fusion. We use galangin and kaempferide, two active chemicals obtained from commonly used plants in Indonesia. Normal physiological parameters were used to a docking and 1000 ps molecular dynamic analysis. The galangin and kaempferide binding sites fluctuatingly changed throughout the experiment. However, chloroquine retains contact with fusion loops due to its lower ligand mobility, whereas both other drugs lose contact with hydrophobic pockets. In contrast, the ligand structure of the two active molecules is more stable. The RMSF simulation of the protein E residues revealed changes of less than 2 Å. In a 1000 ps simulation, all tested compounds form stable complexes with protein E, indicating that the two active compounds may be expected as DENV-2 E protein fusion inhibitors, despite chloroquine inhibiting in a manner that is distinctively tied to its interaction domains.

Keywords: Anti-viral, DENV-2 E protein, Molecular dynamic, RMSF

1. Introduction

Dengue fever, a serious public health issue in tropical and subtropical regions, imposes one of the most severe social and economic costs of any virus transmitted by mosquitoes. Dengue fever is caused by infection with the dengue virus (DENV), a single positive-stranded RNA virus of the family Flaviviridae and genus Flavivirus, as well as other insect-borne viruses such as West Nile Virus and Zika virus, further categorized into four serotypes: DENV-1, -2, -3, -4 [1–5]. These serotypes differ antigenically, and their intricate interactions with the human immune system have hindered efforts to develop a definitive treatment and vaccine [6]. Dengue fever has struck havoc in Indonesia, making it one of the world's worst-affected nations. Indonesia's tropical climate is excellent for the growth of dengue vectors. In addition, the disease has expanded due to the rapid growth of urban and suburban areas. In addition, community migration patterns influence the Indonesian dengue dispersion pattern [7,8]. Since its initial occurrence in 1968, dengue fever has spread throughout Indonesia. All DENV serotypes are prevalent in Indonesia; however, DENV-2 and DENV-3 infections are the most

Received 17 February 2022; revised 14 May 2022; accepted 17 May 2022.
Available online 1 August 2022

* Corresponding author at: Department of Biology, Faculty of Mathematics and Natural Sciences, Universitas Negeri Malang, East Java, Indonesia.
E-mail address: wira.putra.fmipa@um.ac.id (W.E. Putra).

https://doi.org/10.33640/2405-609X.3237

common since they are both endemic in tropical areas, and the principal vector is *Aedes aegepti*, which is also endemic in the tropics [9,10]. Consequently, the death rate continues to decline year after year, from 41% at the outbreak's onset to less than 1% recently. The epidemiological pattern of dengue infection in Indonesia follows a ten-year cycle, with the number of cases reaching a high every ten years [11].

DENV's protein is classified into two major categories: structural proteins and nonstructural proteins. The structure of mature DENV virions is determined by structural proteins, while the replication mechanism of DENV in target cells is determined by nonstructural proteins [12]. Among the DENV structural proteins, the envelope protein (E), which is encased in a lipid bilayer of the viral envelope, is regarded as the most important for antiviral and vaccine development due to its antigenic properties recognized by the immune system, role in the infection cascade, and exposed position in the extracellular environment, which makes it susceptible to small-molecule intervention [6,13]. The DENV-2 E protein is a fusion class II protein that functions through receptor-mediated, clathrin-dependent endocytosis induced by a low pH environment [14–17]. The fusion loops (98–109), the hydrophobic kl hairpin (270–279), and a hydrophobic pocket are some of the key domains in the DENV-2 E protein that may be disrupted by small-molecule inhibitors (130, 135, 193, 198, and 279). These domains are thought to be critical in the DENV fusion mechanism, which is also thought to be the most critical and delicate stage [18–20]. This critical step alters the shape of the E protein's fusion unit, allowing the viral membrane to fuse with the target cell. Antiviral drugs interacting with protein E are highly likely to disrupt this mechanism. This is how antiviral drugs such as those used to treat H1N1 and H3N2 infections perform [18,19,21–23].

Chloroquine, an inexpensive, readily accessible, and well-tolerated lysosomotropic 9-aminoquinoline that is regularly used as an antimalarial medication, has been the topic of a number of drug repositioning studies in the DENV context [24,25]. Chloroquine inhibits low-pH entry steps by preventing endosomal acidification; it also prevents the virus from fusing with the endosomal membrane and interferes with post-translational modifications of newly synthesized proteins required for flavivirus replication such as glycosylation of the transmembranal envelope protein M [13,26,27]. Chloroquine inhibited DENV replication in BHK-21 cells (EC_{90} = 5.04 ± 0.72 μM) but had no impact in a DENV-2 replicon assay, indicating that chloroquine may disrupt the viral entry stage, a hypothesis confirmed by an *in vivo* investigation in *Aotus azarai infulatus* monkeys [28–30]. *In vitro* experiments using U937 cells revealed that dosages of ≥5 μg/mL delivered one hour after infection inhibited DENV replication as well. This study compares galangin and kaempferide as DENV-2 E protein inhibitors with chloroquine, utilizing molecular dynamic parameters [13,25].

2. Materials and methods

2.1. Data retrieval and pre-docking screening

The 3D structure of protein E was retrieved from the primary database, the RSCB PDB (https://www.rcsb.org/) (1OKE), using the AutoDock Vina-compatible PDB file format. The three-dimensional structure is a homodimer with a sequence length of 394 residues and a native ligand of 2-acetamido-2-deoxy-beta-D-glucopyranose on Asn67 and Asn153 residues. PyMol is used to optimize the target protein by eliminating the native ligand from the amino acid sequence. We picked 121 bioactive compounds from PubChem (https://pubchem.ncbi.nlm.nih.gov/) from six different sources (data not shown).

Chloroquine was utilized as a positive control in this research (CID: 2719). All compounds were assessed using the Lipinski rule of five parameters (http://www.scfbio-iitd.res.in/software/drugdesign/lipinski.jsp), then minimized and translated to the AutoDock format using the PyRx tool incorporated with the OpenBabel graphical user interface [31,32].

2.2. Molecular docking process

Docking is accomplished with AutoDock Vina, which is integrated with PyRx (https://pyrx.sourceforge.io/). We used blind docking mechanism, so we look at the whole structure of the target protein [33]. The molecular coverage area is 39.8415 × 56.3282 × 149.8127 Å, and the central coordinates are −12.7517 × 69.0073 × 24.4419 Å. The major docking factors are the molecule's affinity (measured in kcal/mol), the location of the binding site, and the interaction between the protein and the ligands [34].

2.3. Molecular dynamics simulation

To simulate the DENV-2 E protein, the top two ligands with the lowest binding affinity scores and a pharmacological control from the previous experiment, galangin, kaempferide, and chloroquine, were chosen for molecular dynamic simulations

against the DENV-2 E protein, respectively. It was necessary to build the protein and ligand complex structures at physiologically relevant conditions (37 °C, 1 atm, pH 7.4, 0.9 percent salinity) to run 1000 ps simulations. When simulating molecular dynamics, the md run macro program was used, and when analyzing the molecular dynamics data, the md analyze, and md analyeres macro programs were used, respectively.

3. Results

The top two compounds, galangin and kaempferide, exhibited similar affinity values (−8.6 kcal/mol), which was 62.3 percent lower than chloroquine (−5.3 kcal/mol) as a control in blind docking against DENV-2 E protein.

Prior to performing the 3D analysis with PyMol, an alignment procedure was used to compare the structure of the protein-ligand complex before and after simulation using a cycle value of 5.0 and a cutoff value of 2.0. PyMol alignment revealed that none of the three complexes differed by more than 2 Å. The DENV-2 E-galangin complex exhibited the most significant structural deviation (RMSD: 1807 Å), whereas the DENV-2 E-chloroquine complex exhibited the least (RMSD: 1287 Å). Comparing the three post-simulation complexes to the structures before simulation, no major deformations can be observed. In addition, the binding site position and ligand shape did not vary significantly in any of the three complexes visually examined (see Figs. 1 and 2; Table 1).

The two-dimensional plots of the three protein-ligand complex structures before and after molecular dynamic simulation revealed that over 60% of the residues in pre-MD interactions were conserved throughout the three complexes. Galangin and kaempferide interacted with kl hairpin residues (Ile270, Gln271, and Leu277) but not hydrophobic pocket residues. The two compounds' interactions with Gln271 changed significantly. After simulation, the interaction of galangin with Gln271 revealed a 0.31 Å reduction in the hydrogen bond distance compared to before the simulation. Simultaneously, the interaction of kaempferide with Gln271 revealed the insertion of one hydrogen bond with a distance of 2.88 Å after the simulation. Chloroquine maintained a continuous interaction with the fusion loop residues (Asp98, Arg99, Asn103).

To assess each protein-ligand complex flexibility and overall stability, we performed a time-dependent MD simulation at 1000 ps. The graph of the potential energy of the three protein-ligand complexes shows stabilization around $-6.92e^{6}$ after the first 50 ps of simulation until the end of the simulation, indicating that no abnormal behavior occurred in protein-ligand complexes. Also, there is no significant difference between every protein-ligand complex tested. The MD simulation's stability was quantified in terms of deviations and variations from the original structure of the DENV-2 E-ligand complexes. After 50 ps, the RMSD plots of the three protein-ligand complexes revealed that the majority of them remained in a relatively stable form. The mean RMSD values for the three protein-ligand complexes remained within range of 1.58–1.64 Å. The DENV-2 E-kaempferide complex exhibited a more stable plot than the other two complexes, with minor changes and lowered mean and standard deviation values (1.58 ± 0.22 Å). Although the DENV-2 E-chloroquine complex had the most prominent deviation (SD: 0.31 Å), the deviation was not as significant as the deviations for the other two complexes (galangin: 0.29 Å; kaempferide: 0.22 Å). However, after 750 ps, all three exhibit a similar plot pattern, an increase in the RMSD value to the maximum point (galangin: 2.39 Å; kaempferide: 2.02 Å; chloroquine: 2.37 Å), until ultimately dropping below 2 Å in the final 100 ps of the simulation.

The RMSF plot is used to determine the stability and accuracy of protein-ligand complex equilibrium

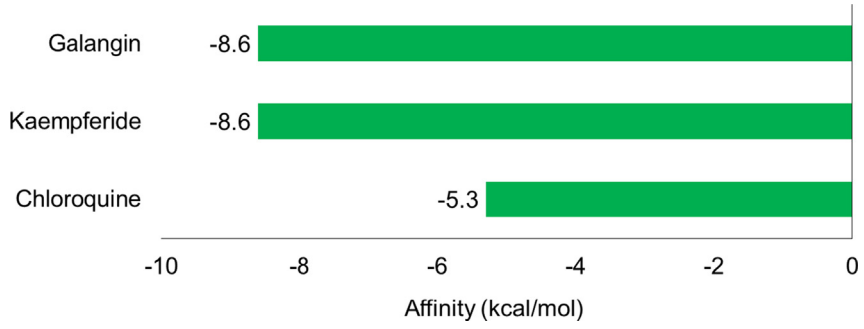

Fig. 1. The comparison of the affinity values of the top two compounds and chloroquine is based on the blind docking results against the prefusion DENV-2 E protein.

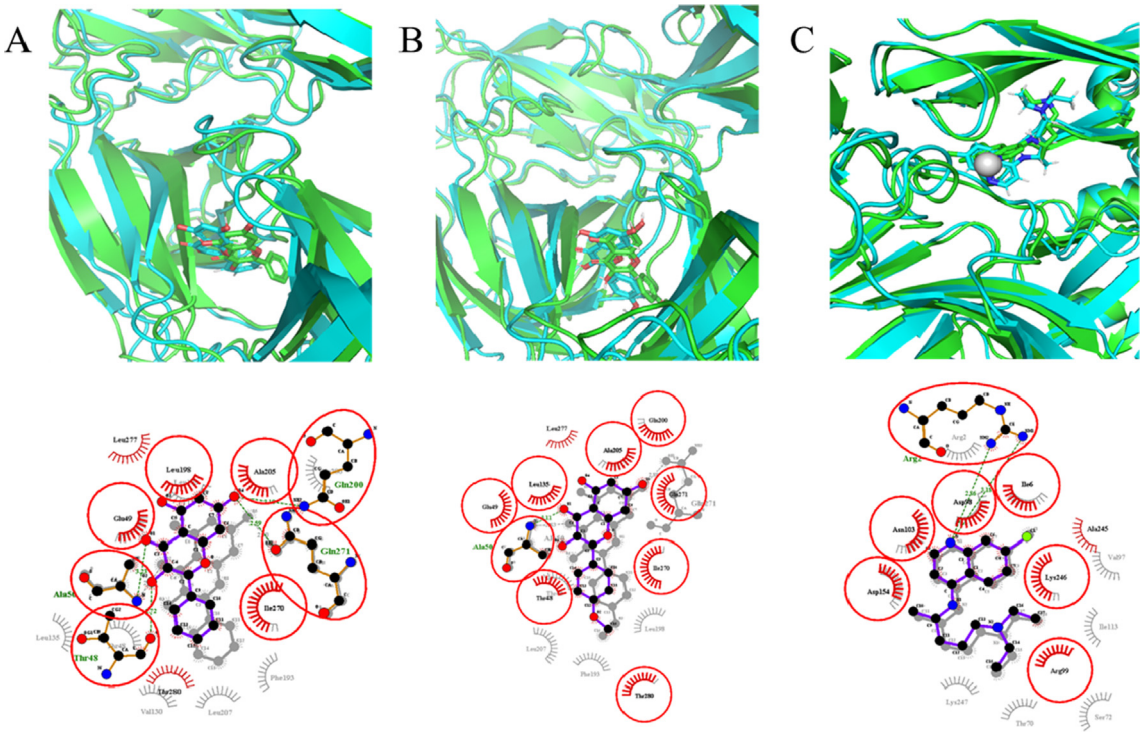

Fig. 2. The 3D and 2D structure visualization of DENV-2 E and (A) galangin, (B) kaempferide, (C) chloroquine complex. The cyan structures in 3D visualization indicate the protein-ligand complex before MD simulation, while the green structures are after MD simulation. The colored diagram in 2D indicates protein-ligand complex after MD, while the greyscale diagram indicates protein-ligand complex before MD.

throughout the simulation. The plots revealed that the target protein residues generally fluctuated below 2 Å in the three protein-ligand complexes studied. Each monomer's N- and C-terminal domains experienced the most remarkable flexibility. There are more significant changes in residues 146–175 and 581–610. However, these two sections do not contain any of the identified vital regions or residues, indicating that the majority of the residues, particularly its critical residues or domains that interact with potent compounds, were stable. The majority of residues that interacted with the tested ligand did not exhibit significantly greater flexibility than the remaining residues in each compound. The fluctuation patterns of the three ligand-protein complexes were highly similar, with no discernible differences.

Chloroquine had the most stable ligand movement plot of the three ligands studied, as seen by its lowest mean value (2.34 ± 0.31 Å). After 100 ps, the chloroquine plot becomes planar but fluctuates between 350 and 950 ps. Both galangin and kaempferide have some degree of active ligand mobility. Galangin demonstrates the trend of the RMSF value, which settled in the 2.5 Å between 400 and 800 ps, although the graph of the galangin ligand movement overall exhibits an increasing tendency throughout the simulation duration. While the kaempferide ligand did not indicate a clear trend like galangin, its value ranged between 3 and 3.5 Å during the simulation period, resulting in the highest mean value of the three ligands examined (2.68 ± 0.55 Å). That value is significantly greater than the value for galangin, whose plot indicates an upward trend over the simulation period (2.46 ± 0.61 Å).

According to the simulation results, the two candidate compounds have a more favorable ligand conformational graph than chloroquine. Galangin is the most stable conformational chart, with a mean deviation of less than one (0.93 ± 0.18 Å). Additionally, the conformational graph of the galangin ligand has a planar trend after 100 ps, with one fluctuation up to 1.5 Å between 600 and 650 ps. Meanwhile, kaempferide exhibits a conformational graph for the first 200 ps that flattens out around 1 Å before rising to approximately 1.5 Å and stabilizing until the simulation period ends. The ligand conformation of kaempferide, which remained at 1.5 Å for 80% of the simulation time, resulted in a mean value equal to that of galangin (1.43 ± 0.31 Å). Chloroquine is the most stable ligand on the ligand movement plot, showing the most significant conformational deviation. The chloroquine conformation plot fluctuates

Table 1. Binding site residues comparison before and after molecular dynamics simulation.

No	Compound	Source	Pre-Molecular Dynamic Simulation		Post-Molecular Dynamic Simulation	
			Amino Acids Residue	Interaction (Å)	Amino Acids Residue	Interaction (Å)
1	Galangin (CID: 5281616)	*Alpinia galanga*	Ile270(B); Phe193(B); Leu207(B); Val130(B); Thr48(B); Leu135(B); Glu49(B); Gln200(B); Leu198(B); Ala205(B); Gln271(B); Ala50(B)	Hydrophobic interaction	Ile270; Thr280; Glu49; Leu198; Leu277; Ala205; Gln200; Gln271; Thr48; Ala50	Hydrophobic interaction
			Gln271(B)	Hydrogen bond (2.90)	Gln200	Hydrogen bond (3.18)
			Ala50(B)	Hydrogen bond (2.88)	Gln271	Hydrogen bond (2.59)
					Thr48	Hydrogen bond (2.72)
					Ala50	Hydrogen bond (3.23)
2	Kaempferide (CID: 5281666)	*Alpinia galanga*	Ile270(B); Leu198(B); Leu207(B); Phe193(B); Thr280(B); Thr48(B); Glu49(B); Leu135(B); Gln200(B); Ala205(B); Gln271(B); Ala50(B)	Hydrophobic interaction	Gln200; Gln271; Ile270; Thr280; Thr48; Glu49; Ala50; Leu277; Ala205	Hydrophobic interaction
			Gln271(B)	Hydrogen bond (2.88)	Ala50	Hydrogen bond (3.11)
			Ala50(B)	Hydrogen bond (2.83)		
3	Chloroquine (CID: 2719)	Antiviral drug (control)	Val97(A); Ile113(A); Arg99(A); Ser72(A); Thr70(A); Lys247(A); Asp154(B); Asn103(A); Asp98(A); Arg2(B); Ile6(B)	Hydrophobic interaction	Ile6; Ala245; Lys246; Arg99; Asp154; Asn103; Asp98; Arg2	Hydrophobic interaction
					Arg2	Hydrogen bond (2.86) Hydrogen bond (3.18)

between 1.5 and 2 Å during the first 250 ps before stabilizing at 1.5 Å for the remainder of the simulation time, resulting in chloroquine having the most significant mean deviation value of the three ligands studied (1.60 ± 0.23 Å). Additionally, chloroquine had the highest maximum value (2.01 Å) of all (Figs. 3, 4, and 5).

The 1000 ps SASA simulation revealed that none of the three protein-ligand complexes expanded rapidly over the simulation period. The graphs of SASA values for the DENV-2 E-galangin and the DENV-2 E-chloroquine complexes are generally flat with oscillations around 36500 $Å^2$, but the graphs of the DENV-2 E-galangin and E-chloroquine complexes begin to diverge about 700 ps when galangin hits its maximum SASA value, and chloroquine remains flat. The E5-kaempferide complex has a similar SASA chart pattern to the other two ligands for the first 250 ps, but after 250 ps, the SASA complex value continually displays a decreasing trend, eventually falling below 36000 $Å^2$ at the end of the simulation time. However, none of them indicated a significant increase in SASA levels over a short period.

The Rg values for the DENV-2 E protein's backbone atoms were determined and plotted against simulation time. Throughout the 1000 ps simulation, the three complexes displayed radius fluctuations in the range 43.1–44.1 Å, and none of them expressed a horizontal graphic pattern showing the stability of the Rg value. The three complexes have a mean Rg value of roughly 43–44 Å, with the DENV-2 E-galangin complex having the highest mean value (43.82 ± 0.17 Å) and kaempferide having the lowest mean value (43.59 ± 0.17 Å). Based on the observations, the three complexes' maximum and minimum Rg values are roughly comparable. Galangin, kaempferide, and chloroquine have maximum Rg values of 44.10, 43.92, and 43.95 Å, respectively, whereas galangin, kaempferide, and chloroquine have minimum Rg values of 43.14, 43.13, and 43.14 Å, respectively.

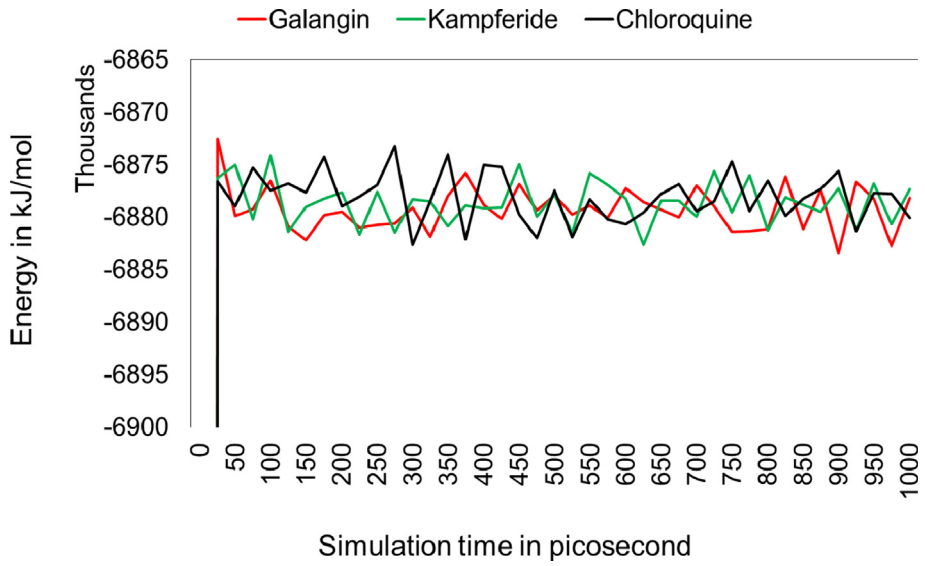

Fig. 3. Potential energy for prefusion envelope protein complex with galangin (red line), kaempferide (green line), and chloroquine (black line) over a 1000 ps of simulation.

For 1000 ps, the intramolecular hydrogen bond plot revealed that the three protein-ligand complexes changed less than 10% throughout the simulation time. While none of the protein-ligand complexes exhibited a horizontal visual pattern, the DENV-2 E-chloroquine complex did exhibit a consistent pattern of hydrogen bond fluctuation throughout the simulation. Meanwhile, galangin

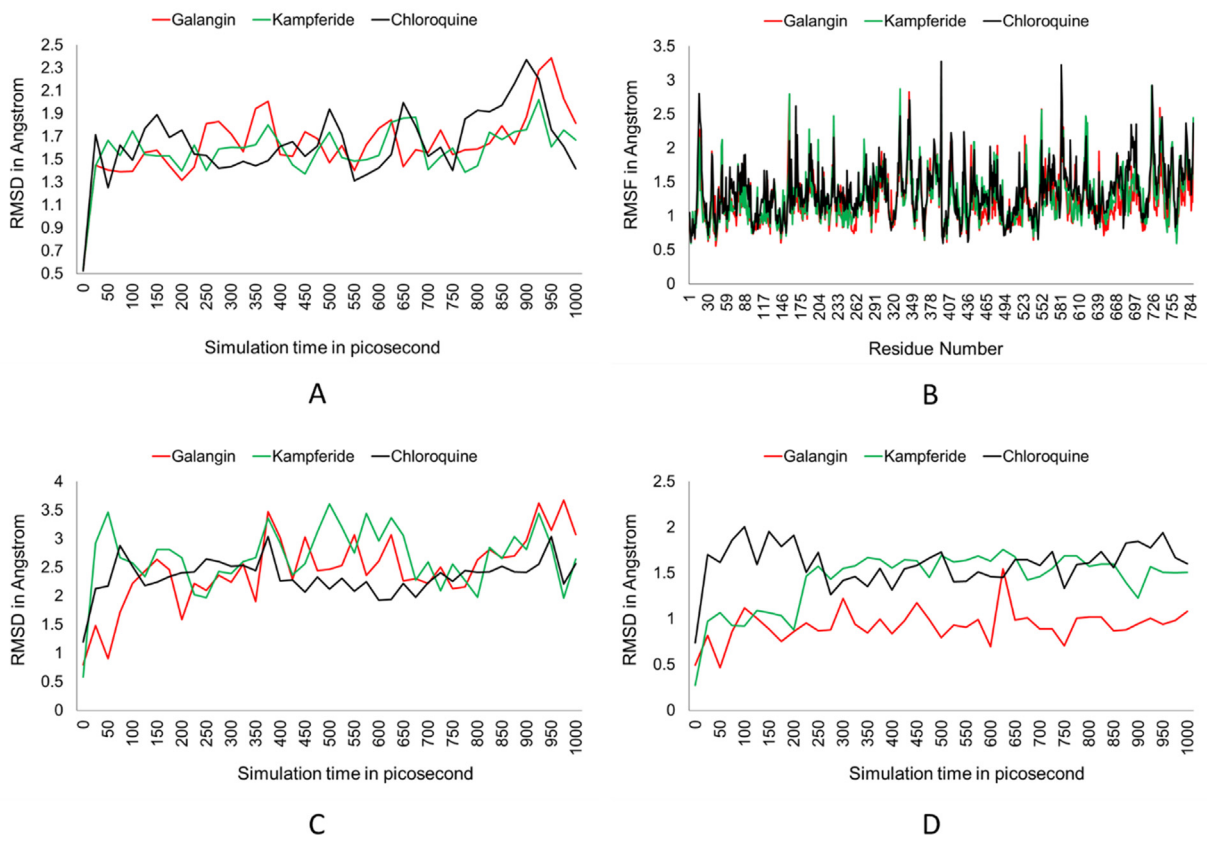

Fig. 4. (A) RMSD plot, (B) RMSF plot, (C) ligand movement plot, and (D) ligand conformation plot for galangin (red line), kaempferide (green line), and chloroquine (black line) complexes over a 1000 ps of simulation.

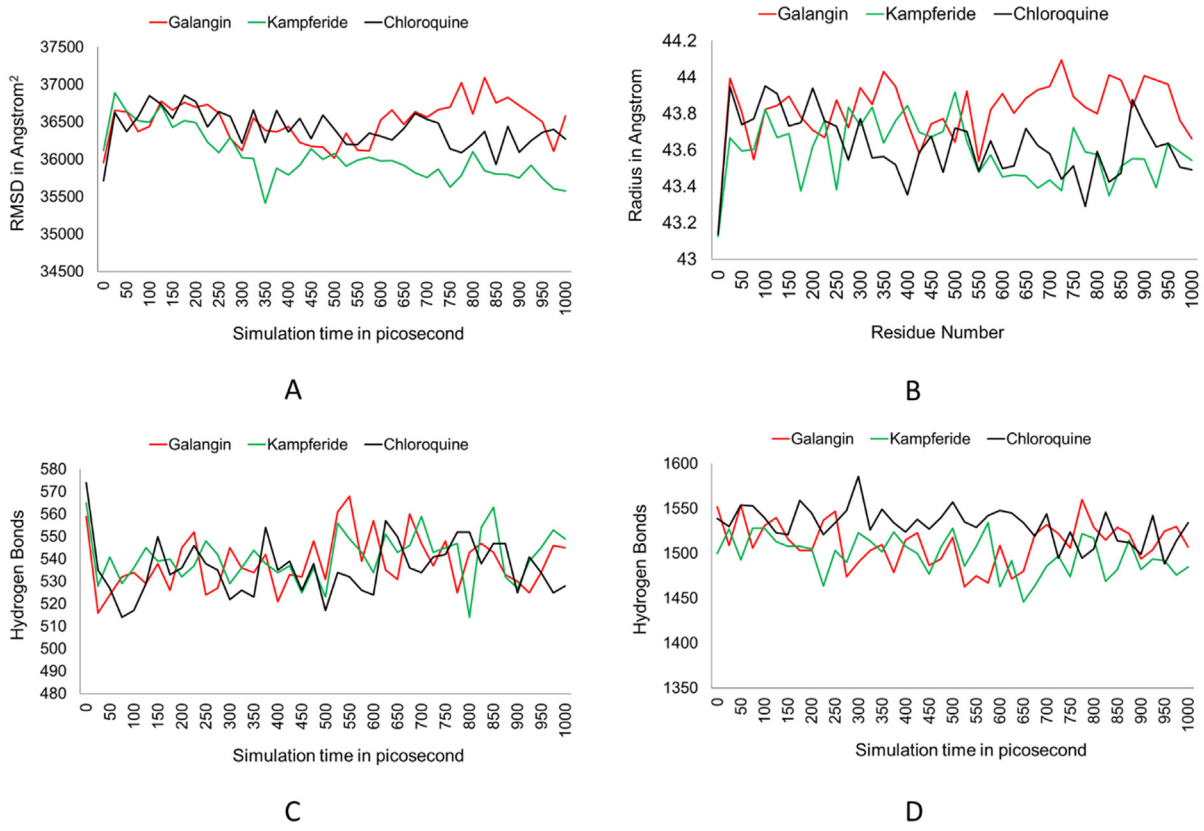

Fig. 5. (A) SASA plot, (B) Rg plot, (C) intramolecular hydrogen bond plot, and (D) protein-solvent hydrogen bond plot for galangin (red line), kaempferide (green line), and chloroquine (black line) complexes over a 1000 ps of simulation.

and kaempferide exhibited a more pronounced pattern of instability after 500 ps, whereas earlier, the two complexes, particularly DENV-2 E-kaempferide, fluctuated within the 530–540 Å range. In the protein-solvent hydrogen bond diagram, a similar trend was seen. The DENV-2 E-chloroquine complex exhibited a consistent trend, particularly between 300 and 700 ps, but the kaempferide and galangin complex fluctuated between 1450 and 1550 Å and lacked a stable visual pattern throughout the 1000 ps simulation period. Except for galangin, both complexes exhibited a declining protein-solvent hydrogen bond plot pattern during the course of the simulation. However, there were no

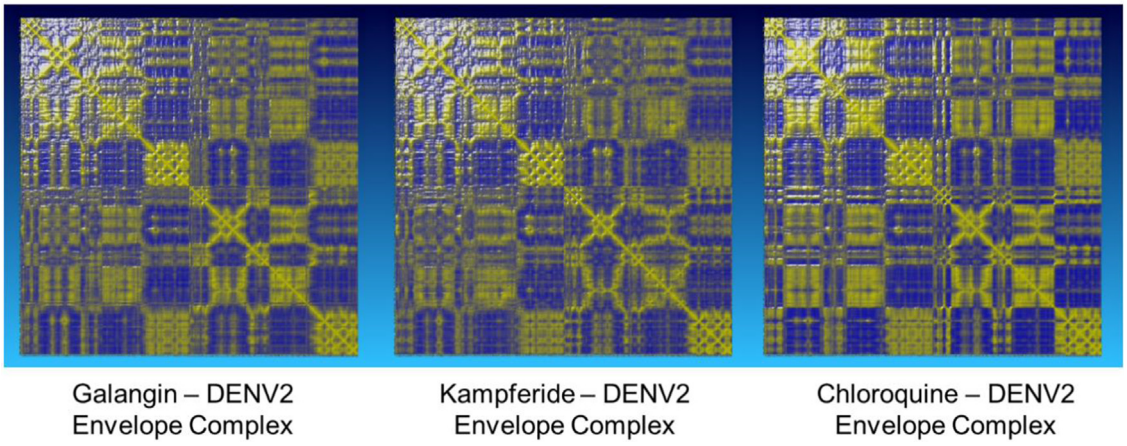

Fig. 6. Dynamic cross-correlation matrix for each protein-ligand complex. Yellow represents correlated motions, and blue represents anticorrelated motions.

significant changes in the two hydrogen bond graphs associated with the three protein complexes.

The DCCM graphs demonstrate that the three protein-ligand complexes exhibit dynamic movement patterns that are almost similar. The DCCM for the E protein alone demonstrates statistically significant positive correlations within each of the three domains I, II, and III of the E protein. Domains II and III exhibit both positive and negative correlations in their atomic fluctuations, but the movements of EDI are only weakly associated with the motions of EDII and EDIII. EDII and EDIII exhibit both positive and negative correlations in their atomic fluctuations. Although the chloroquine complex is very dynamic, the galangin and kaempferide complexes exhibit a similar degree of dynamism and are either stiffer or less elastic than the chloroquine complex (see Fig. 6).

4. Discussion

The protein envelope present on the surface of DENV is one of the critical proteins involved in the first process of infection with Flaviviruses such as DENV, as it facilitates receptor recognition and fusion of the viral membrane with target cells such as dendritic cells [16,35]. The envelope protein in mature DENV-2 virions is dimer protein complexes that lays flat on the viral surface and must undergo conformational changes to interact with the cell receptor and enable fusion, referred to as the prefusion stage [36,37]. When mature DENV-2 new virions are exposed to particular conditions, most notably a low pH environment, they undergo a conformational change to a post-fusion state and initiate the fusion sequences [14,18].

One of the most significant and naturally active flavonoids is galangin, also known as 3,5,7-trihydroxyflavone. It's a polyphenolic substance derived primarily from *Alpinia galanga* and *Alpinia officinarum* rhizome [38–40]. Galangin comprises two benzene rings connected by a C3 aliphatic chain comprising a heterocyclic pyran ring with a 2,3-double bond with a 3-hydroxyl group in the C-ring and 5,7-dihydroxyl groups in the A-ring, but no hydroxyl group in the B-ring [41–43]. It's been suggested as an anticancer agent since it suppresses proliferation, causes apoptosis, promotes autophagy in carcinoma cells, and is an antioxidant because it's a potent scavenger of free radicals like singlet oxygen and superoxide anion [44,45].

Kaempferide is a monomethoxyflavone that is the 4′-O-methyl derivative of kaempferol—a flavonol that belongs to the family of flavonoids with a hydroxyl group on carbon 3 of the core oxygen-containing 6-member ring, and it is abundant in *A. galanga* and *Kaempferia galanga* [39,46–49]. It's also usually suggested as an anti-inflammatory and antioxidant [50–52]. Because most studies are focused on kaempferol, research on kaempferide is currently limited. According to one research, kaempferide had a higher affinity for protein than its unmethylated equivalent [53].

The study of galangin and kaempferide's antiviral effects on flaviviruses is still in its early stages. Galangin and kaempferide, according to one of them, can both behave as entry and translation inhibitors of Zika virus (ZIKV) by inhibiting NS2B-NS3 protease with EC_{50} values of 25.68 ± 9.17 μM and 7.18 ± 2.16 μM, respectively. The key benefit is that they have no cytotoxic impact on the Vero cell type utilized as a host, even at greater doses [54]. Because DENV-2 is closely linked to ZIKV, with a virtually comparable entry mechanism [55–57] and a highly conserved NS2B–NS3 protease across flaviviruses, this discovery might indicate that a similar impact could occur [58,59].

Kaempferide and galangin have lower affinity values than chloroquine, suggesting that their interactions with DENV-2 E are more stable and that their likelihood to interact with the target protein is better than the control [34,60,61]. The docking results with a negative value reflect a spontaneous interaction between the ligand and the target protein when the ligand–protein complex achieves an equilibrium point at constant pressure and temperature, which is mimicked in the docking process [61–63].

Galangin retained interaction with kl hairpin residues but lost contact with the hydrophobic pocket of the DENV-2 E protein over the simulation period. Because the hydrophobic pocket acts as a hinge in the fusion process, the loss of contact with the hydrophobic pocket residues is considered to inhibit the conformational transition process from the prefusion state to the post-fusion state [14,20]. Galangin, on the other hand, retains contact with the kl hairpin residues, which is the trigger area in the conformational change process, indicating that the fusion inhibition mechanism moves to the very early stage or the initiating step of fusion [18,20,64,65]. It is predicted that galangin's interaction with kl hairpin causes premature triggering and prevents fusion in a low pH environment [66]. The exact inhibitory mechanism is believed to exist in the DENV-2 E-kaempferide protein complex, as kaempferide's interaction pattern in simulation is comparable to galangin. Throughout the simulation period, chloroquine maintains a lasting contact with the fusion peptide residues of the DENV-2 E protein

and is the only chemical that interacts directly with fusion peptide residues. This contact is considered to disrupt the DENV fusion process with the target cells since the fusion peptide acts as the primary anchor for attaching the DENV virion to the target cell's membrane when the fusion stage has initiated [18,20]. If the DENV-host fusion mechanism is examined chronologically, the process blocked by galangin and kaempferide happened prior to the phase stopped by chloroquine, which may have a little higher likelihood. Combining galangin/kaempferide potentials with chloroquine via a complementary therapeutic mechanism, on the other hand, may offer some redundancy, increasing the likelihood of fusion inhibition.

The potential energy plots of the three complexes displayed a remarkably similar stability pattern, particularly after passing through a time of 50 ps, indicating that the electrostatic and van der Waals interactions of the three complexes were in equilibrium, implying that no abnormalities occurred during the simulation process [67,68]. The RMSD value indicates that the kaempferide complex is more stable than galangin or chloroquine, as demonstrated by the simulated complex's lowest mean deviation. The results, however, are not significantly different from those obtained with the other two protein-ligand complexes, showing that the stability of the three protein-ligand complexes examined remains comparable. Visual confirmation and the PyMOL's alignment RMSD values, which are less than 2 Å, also suggest a similar result: the three complexes examined did not undergo significant deformation during the simulation process, indicating that they are generally stable [69,70]. The RMSF figure revealed no outliers in the domain residues interacting with the three potent compounds (kl hairpin or fusion peptide) [71–73].

When the three compounds are examined before and after the simulation, they appear not jettisoned from their initial binding pocket; only they seem to rotate less than 90°. The two-dimensional representation likewise reveals comparable results characterized by a high level of conserved residues throughout the simulation time (>50%). These two results show that each of the three compounds tested has occupied its optimal binding location [69,74]. The movement and conformational changes observed in the movement and conformational plots are believed to be generated by each ligand altering its conformation and location in response to the dynamics of its binding site during the simulation process [74–76].

The solvent accessibility surface area is the surface area of a bimolecular that is accessible to solvent molecules. In general, protein complexes that are not sufficiently compact undergo fast unfolding, as evidenced by a rapid increase in the SASA value over a short period [77,78]. There were no signs of denaturation in any of the three complexes examined. Galangin and chloroquine both have a reasonably flat graph pattern. However, the chloroquine plot also has a downward trend, while kaempferide exhibits a steadily declining graph pattern. The reduced value of SASA, particularly in the E-kaempferide complex, indicates that it has shrunk in size relative to the native structure, owing to the target protein's interaction with kaempferide [79]. The radius gyration analysis, which quantifies the protein structure's compactness, indicates that the kaempferide and chloroquine complexes are stiffer than the galangin complex since both have a lower Rg value than galangin [80,81].

Hydrogen bond analysis indicated significant changes in both values, suggesting that the three protein-ligand complexes moved continuously over the simulation time to achieve equilibrium [82,83]. The three complexes had comparable graphs, and both exhibited intramolecular fluctuation after 500 ps, indicating that the three proteins' movement grew more intensive in the second part of the simulation. These motions, however, do not suggest that the protein complexes have been denatured. The protein-solvent hydrogen bond plot exhibits a similar trend similar to the SASA and Rg values plots. Because the available donor and acceptor atoms are assigned to create intramolecular hydrogen bonds in shrunken protein structures, the decreased surface area also decreases the likelihood of target protein residues making hydrogen bonds with water [84–86].

The DCCM analysis indicates that all protein-ligand complexes exhibit correlated motion patterns almost indistinguishable from one another. Attributable to its structure, which is dominated by β-sheets, the highly dynamic E protein is predicted to be due to its function as a fusion protein, which is more or less related to its structure. This dynamic is hypothesized to be caused by the protein's alternating arrangement of key domain residues [20,87,88]. Given that both the galangin and kaempferide complexes demonstrate a similar degree of dynamism and are either stiffer or less elastic than the chloroquine complex, it is reasonable to predict that both complexes are relatively more stable compared to chloroquine.

5. Conclusion

Since the envelope protein is a critical component of the DENV fusion process, we are targeting it with

two active natural compounds: galangin and kaempferide. There were fluctuations in galangin and kaempferide binding sites throughout the simulated period. Both drugs keep contact with kl hairpin residues but lose touch with hydrophobic pockets, but chloroquine has considerably lower ligand mobility and retains contact with fusion loops. On the other hand, the two possible compounds have a more stable ligand conformation. The RMSF simulation demonstrated that the crucial protein E residue remained stable with changes of less than 2 Å. Additionally, the potential energy, SASA, hydrogen bond, Rg, and DCCM graphs demonstrate that the three compounds form a stable complex with protein E during a 1000 ps simulation, indicating that the two potential compounds have the potential to act as DENV-2 E protein fusion inhibitors even though chloroquine inhibits distinctly is related to its interaction domains. Additional research is necessary to validate this study's prediction and to advance the development of these compounds as antiviral agents that specifically target the DENV E protein.

Author's contribution

Arief Hidayatullah provided the theoretical framework, performed molecular docking, wrote and revised the article. Wira Eka Putra conceptualized the central research idea, provided the theoretical framework, performed molecular dynamic simulations, wrote and revised the article. Muhaimin Rifa'i conceptualized the central research idea, provided the discussion, and revised the article. Sustiprijatno provided the theoretical framework and revised the article. Diana Widiastuti, Muhammad Fikri Heikal, Hendra Susanto, Wa Ode Salma, and Hilal Mulyadi provided the discussion and revised the article. All authors anchored the review, revisions and approved the article submission.

Acknowledgements

This study was funded by PNBP Universitas Negeri Malang with contract number 5.3.619/UN32.14.1/LT/2021 and 5.3.517/UN32.14.1/LT/2021 (Wira Eka Putra). All authors thank Universitas Negeri Malang and Computational Laboratory, Brawijaya University for supported and facilitated this study.

References

[1] I.M.S. Utama, N. Lukman, D.D. Sukmawati, B. Alisjahbana, A. Alam, D. Murniati, I.M.G.D.L. Utama, D. Puspitasari, H. Kosasih, I. Laksono, M. Karyana, M.R. Karyanti, M.M.D.E.a.H. Hapsari, N. Meutia, C.J. Liang, W.N. Wulan, C-Y. Lau, K.T.M. Parwati, Dengue viral infection in Indonesia: Epidemiology, diagnostic challenges, and mutations from an observational cohort study, PLOS Neglected Tropical Diseases. 13 (2019) 1–19.

[2] R.A. Tahir, H. Wu, M.A. Rizwan, T.H. Jafar, S. Saleem, S.A. Sehgal, Immunoinformatics and molecular docking studies reveal potential epitope-based peptide vaccine against DENV-NS3 protein, J Theoret Biol. 459 (2018) 162–170.

[3] T. Warkentien, Dengue fever: historical perspective and the global response, J Infect Dis Epidemiol. 2 (2016) 1–6.

[4] V. Nayak, M. Dessau, K. Kucera, K. Anthony, M. Ledizet, Y. Modis, Crystal structure of dengue virus type 1 envelope protein in the postfusion conformation and its implications for membrane fusion, J Virol. 83 (2009) 4338–4344.

[5] C. Guzmán, A. Calderón, S. Mattar, L. Tadeu-Figuereido, J. Salazar-Bravo, N. Al-vis-Guzmán, E.Z. Martinez, M. González, Chapter 6 - ecoepidemiology of alphaviruses and flaviviruses, in: M.M. Ennaji (Ed.), Emerging and Reemerging Viral Pathogens, Academic Press, 2020: pp. 101–125.

[6] N. Coconi-Linares, E. Ortega-Dávila, M. López-González, J. García-Machorro, J. García-Cordero, R.M. Steinman, L. Cedillo-Barrón, M.A. Gómez-Lim, Targeting of envelope domain III protein of DENV type 2 to DEC-205 receptor elicits neutralizing antibodies in mice, Vaccine. 31 (2013) 2366–2371.

[7] M. Nadjib, E. Setiawan, S. Putri, J. Nealon, S. Beucher, S.R. Hadinegoro, V.Y. Permanasari, K. Sari, T.Y.M. Wahyono, E. Kristin, D.N. Wirawan, H. Thabrany, Economic burden of dengue in Indonesia, PLoS Negl Trop Dis. 13 (2019) 1–14.

[8] B. Haryanto, Indonesia dengue fever: status, vulnerability, and challenges, in: A.J. Rodriguez-Morales (Ed.), Current Topics in tropical emerging diseases and travel medicine, 5, IntechOpen, 2018: pp. 81–92.

[9] S. Masyeni, B. Yohan, R.T. Sasmono, Concurrent infections of dengue virus serotypes in Bali, Indonesia, BMC Res Notes. 12 (2019) 1–6.

[10] L.C. Katzelnick, J. Coloma, E. Harris, Dengue: knowledge gaps, unmet needs, and research priorities, The Lancet Infect. 17 (2017) 88–100.

[11] M.R. Karyanti, S.R. Hadinegoro, Perubahan epidemiologi demam berdarah dengue di Indonesia, Sari Pediatri. 10 (2016) 424–432.

[12] H. Norazharuddin, N.S. Lai, Roles and prospects of dengue virus non-structural proteins as antiviral targets: an easy digest, Malays J Med Sci. 25 (2018) 6–15.

[13] K.J.S. Farias, P.R.L. Machado, R.F. de A. Junior, A.A. de Aquino, B.A.L. da Fonseca, Ana Alice de Aquino, Benedito Antônio Lopes da Fonseca, Chloroquine interferes with dengue-2 virus replication in U937 cells, Microbiol Immunol. 58 (2014) 318–326.

[14] M.M.F. Alen, D. Schols, Dengue virus entry as target for antiviral therapy, Trop Med. (2012) (2012) 1–13.

[15] S. Butrapet, T. Childers, K.J. Moss, S.M. Erb, B.E. Luy, A.E. Calvert, C.D. Blair, J.T. Roehrig, C.Y.H. Huang, Amino acid changes within the E protein hinge region that affect dengue virus type 2 infectivity and fusion, Virology. 413 (2011) 118–127.

[16] J.M. Smit, B. Moesker, I. Rodenhuis-Zybert, J. Wilschut, Flavivirus cell entry and membrane fusion, Viruses. 3 (2011) 160–171.

[17] M. de Wispelaere, W. Lian, S. Potisopon, P.-C. Li, J. Jang, S.B. Ficarro, M.J. Clark, X. Zhu, J.B. Kaplan, J.D. Pitts, T.E. Wales, J. Wang, J.R. Engen, J.A. Marto, N.S. Gray, P.L. Yang, Inhibition of flaviviruses by targeting a conserved pocket on the viral envelope protein, Cell Chem Biol. 25 (2018) 1006–1016.

[18] D.E. Klein, J.L. Choi, S.C. Harrison, Structure of a dengue virus envelope protein late-stage fusion intermediate, J Virol. 87 (2013) 2287–2293.

[19] A. Rouvinski, W. Dejnirattisai, P. Guardado-Calvo, M.-C. Vaney, A. Sharma, S. Duquerroy, P. Supasa, W. Wongwiwat, A. Haouz, G. Barba-Spaeth, J. Mongkolsapaya, F.A. Rey, G.R. Screaton, Covalently linked dengue virus envelope glycoprotein dimers reduce exposure of the immunodominant fusion loop epitope, Nat Commun. 8 (2017) 1–12.
[20] A. Rouvinski, W. Dejnirattisai, P. Guardado-Calvo, M.-C. Vaney, A. Sharma, S. Duquerroy, P. Supasa, W. Wongwiwat, A. Haouz, G. Barba-Spaeth, J. Mongkolsapaya, F.A. Rey, G.R. Screaton, Structure-Based Design of Antivirals against Envelope Glycoprotein of Dengue Virus, Viruses. 12 (2020) 1–23.
[21] M. Shah, A. Wadood, Z. Rahman, T. Husnain, Interaction and Inhibition of Dengue Envelope Glycoprotein with Mammalian Receptor DC-Sign, an In-Silico Approach, PLoS One. 8 (2013) 1–10.
[22] S.C. Harrison, Viral membrane fusion, Virology. 480 (2015) 498–507.
[23] X. Wang, R. Cao, H. Zhang, J. Liu, M. Xu, H. Hu, Y. Li, L. Zhao, W. Li, X. Sun, X. Yang, Z. Shi, F. Deng, Z. Hu, W. Zhong, M. Wang, The anti-influenza virus drug, arbidol is an efficient inhibitor of SARS-CoV-2 in vitro, Cell Discov. 6 (2020) 1–5.
[24] X. Wang, R. Cao, H. Zhang, J. Liu, M. Xu, H. Hu, Y. Li, L. Zhao, W. Li, X. Sun, X. Yang, Z. Shi, F. Deng, Z. Hu, W. Zhong, M. Wang, A randomized controlled trial of chloroquine for the treatment of dengue in vietnamese adults, PLoS Negl Trop Dis. 4 (2010) 1–12.
[25] L. Botta, M. Rivara, V. Zuliani, M. Radi, Drug repurposing approaches to fight Dengue virus infection and related diseases, Front Biosci (Landmark Ed). 23 (2018) 997–1019.
[26] V.B. Randolph, G. Winkler, V. Stollar, Acidotropic amines inhibit proteolytic processing of flavivirus prM protein, Virology. 174 (1990) 450–458.
[27] J. Verma, N. Subbarao, M.S. Rajala, Rajala, envelope proteins as antiviral drug target, J Drug Target. 28 (2020) 1046–1052.
[28] S. Boonyasuppayakorn, E.D. Reichert, M. Manzano, K. Nagarajan, R. Padmanabhan, Amodiaquine, an antimalarial drug, inhibits dengue virus type 2 replication and infectivity, Antiviral Res. 106 (2014) 125–134.
[29] M.A.M. Behnam, C. Nitsche, V. Boldescu, C.D. Klein, The medicinal chemistry of dengue virus, J Med Chem. 59 (2016) 5622–5649.
[30] K.J.S. Farias, P.R.L. Machado, J.A.P.C. Muniz, A.A. Imbeloni, B.A.L. da Fonseca, Antiviral activity of chloroquine against dengue virus type 2 replication in aotus monkeys, Viral Immunol. 28 (2015) 161–169.
[31] B. Jayaram, T. Singh, G. Mukherjee, A. Mathur, S. Shekhar, V. Shekhar, Sanjeevini: a freely accessible web-server for target directed lead molecule discovery, BMC Bioinf. 13 (2012) 1–13.
[32] H. Mirzaei, S. Zarbafian, E. Villar, S. Mottarella, D. Beglov, S. Vajda, I.Ch. Paschalidis, P. Vakili, D. Kozakov, Energy minimization on manifolds for docking flexible molecules, J Chem Theory Comput. 11 (2015) 1063–1076.
[33] N.M. Hassan, A.A. Alhossary, Y. Mu, C.-K. Kwoh, Protein-Ligand blind docking using quickvina-w with inter-process spatio-temporal integration, Sci Rep. 7 (2017) 1–13.
[34] O. Trott, A.J. Olson, Improving the speed and accuracy of docking with a new scoring function, efficient optimization, and multithreading, J Comput Chem. 31 (2009) 455–461.
[35] T. Hu, Z. Wu, S. Wu, S. Chen, A. Cheng, The key amino acids of E protein involved in early flavivirus infection: viral entry, Virol J. 18 (2021) 136 1–13612.
[36] Y. Modis, S. Ogata, D. Clements, S.C. Harrison, A ligand-binding pocket in the dengue virus envelope glycoprotein, Proc Nat Acad Sci. 100 (2003) 6986–6991.
[37] C. De La Guardia, R. Lleonart, Progress in the identification of dengue virus entry/fusion inhibitors, Biomed Res Int. 2014 (2014) 1–13.
[38] A. Kaur, R. Singh, C.S. Dey, S.S. Sharma, K.K. Bhutani, I.P. Singh, Bhutani, Inder Pal Singh, Antileishmanial phenylpropanoids from Alpinia galanga (Linn.) Willd, Indian J Exp Biol. 48 (2010) 314–317.
[39] W. Yan, W. Ying, L. Zhi Hua, W. Cheng Fang, W. Jian Yu, L. Xiao Lan, W. Ping Juan, Z. Zhao Feng, D. Shu Shan, H. Dong Ye, D. Zhi Wei, Composition of the essential oil from Alpinia galanga rhizomes and its bioactivity on Lasioderma serricorne, Bull Insectol. 67 (2014) 247–254.
[40] L. Tao, Z.-T. Wang, E.-Y. Zhu, Y.-H. Lu, D.-Z. Wei, HPLC analysis of bioactive flavonoids from the rhizome of Alpinia officinarum, S Aft J Bot. 72 (2006) 163–166.
[41] D. Fang, Z. Xiong, J. Xu, J. Yin, R. Luo, Chemopreventive mechanisms of galangin against hepatocellular carcinoma: A review, Biomed Pharmacother. 109 (2019) 2054–2061.
[42] H.N. Lee, S.A. Shin, G.S. Choo, H.J. Kim, Y.S. Park, B.S. Kim, S.K. Kim, S.D. Cho, J.S. Nam, C.S. Choi, J.H. Che, B.K. Park, J.Y. Jung, Anti-inflammatory effect of quercetin and galangin in LPS-stimulated RAW264.7 macrophages and DNCB-induced atopic dermatitis animal models, Int J Mol Med. 41 (2018) 888–898.
[43] S. Kumar, A.K. Pandey, Chemistry and biological activities of flavonoids: an overview, Sci World J. (2013) (2013) 1–16.
[44] A.S. Sivakumar, C.V. Anuradha, Effect of galangin supplementation on oxidative damage and inflammatory changes in fructose-fed rat liver, Chemico-Bio Interact. 193 (2011) 141–148.
[45] X. Li, Y. Wang, Y. Xiong, J. Wu, H. Ding, X. Chen, L. Lan, H. Zhang, Galangin induces autophagy via deacetylation of LC3 by SIRT1 in HepG2 Cells, Sci Rep. 6 (2016) 1–8.
[46] H.-L. Li, S.-M. Li, Y.-H. Luo, W.-T. Xu, Y. Zhang, T. Zhang, D.-J. Zhang, C.-H. Jin, Kaempferide induces G0/G1 phase arrest and apoptosis via ROS-mediated signaling pathways in A549 human lung cancer cells, Nat Prod Commun. 15 (2020) 1–13.
[47] R. Shukla, V. Pandey, G.P. Vadnere, S. Lodhi, Chapter 18 - role of flavonoids in management of inflammatory disorders, in: R.R. Watson, V.R. Preedy (Eds.), Bioactive Food as Dietary Interventions for Arthritis and Related Inflammatory Diseases, Second Edition, Academic Press, 2019: pp. 293–322.
[48] I. Horibe, Y. Satoh, Y. Shiota, A. Kumagai, N. Horike, H. Takemori, S. Uesato, S. Sugie, K. Obata, H. Kawahara, Y. Nagaoka, Induction of melanogenesis by 4′-O-methylated flavonoids in B16F10 melanoma cells, J Nat Med. 67 (2013) 705–710.
[49] S. Munda, P. Saikia, M. Lal, Chemical composition and biological activity of essential oil of Kaempferia galanga : a review, J Essent Oil Res. 30 (2018) 303–308.
[50] X. Ma, Y. Tian, K. Xue, Y. Huai, S. Patil, X. Deng, Q. Hao, D. Li, Z. Miao, W. Zhang, A. Qian, Kaempferide enhances antioxidant capacity to promote osteogenesis through FoxO1/β-catenin signaling pathway, Eur J Pharmacol. 911 (2021) 1–13.
[51] H. Tang, Q. Zeng, N. Ren, Y. Wei, Q. He, M. Chen, P. Pu, Kaempferide improves oxidative stress and inflammation by inhibiting the TLR4/IκBα/NF-κB pathway in obese mice, Iran J Basic Med Sci. 24 (2021) 493–498.
[52] T. Yan, B. He, M. Xu, B. Wu, F. Xiao, K. Bi, Y. Jia, Kaempferide prevents cognitive decline via attenuation of oxidative stress and enhancement of brain-derived neurotrophic factor/tropomyosin receptor kinase B/cAMP response element-binding signaling pathway, Phytother Res. 33 (2019) 1065–1073.
[53] H. Cao, X. Jing, D. Wu, Y. Shi, Methylation of genistein and kaempferol improves their affinities for proteins, International J Food Sci Nutr. 64 (2013) 437–443.
[54] M. Zou, H. Liu, J. Li, X. Yao, Y. Chen, C. Ke, S. Liu, Structure-activity relationship of flavonoid bifunctional inhibitors against Zika virus infection, Biochem Pharmacol. 177 (2020) 1–9.
[55] M. Laureti, D. Narayanan, J. Rodriguez-Andres, J.K. Fazakerley, L. Kedzierski, Flavivirus Receptors: Diversity, Identity, and Cell Entry, Front Immunol. 9 (2018) 1–11.

[56] R.C. Coldbeck-Shackley, N.S. Eyre, M.R. Beard, The Molecular interactions of ZIKV and DENV with the Type-I IFN response, Vaccines (Basel). 8 (2020) 1–20.
[57] A. Agrelli, R.R. de Moura, S. Crovella, L.A.C. Brandão, ZIKA virus entry mechanisms in human cells, Infect Genet Evol. 69 (2019) 22–29.
[58] Z. Li, J. Zhang, H. Li, Chapter 7 - Flavivirus NS2B/NS3 Protease: Structure, Function, and Inhibition, in: S.P. Gupta (Ed.), Viral Proteases and Their Inhibitors, Academic Press, 2017: 163–188.
[59] D. Aguilera-Pesantes, L.E. Robayo, P.E. Méndez, D. Mollocana, Y. Marrero-Ponce, F.J. Torres, M.A. Méndez, Discovering key residues of dengue virus NS2b-NS3-protease: New binding sites for antiviral inhibitors design, Biochem Biophys Res Commun. 492 (2017) 631–642.
[60] T. Pantsar, A. Poso, Binding Affinity via Docking: Fact and Fiction, Molecules. 23 (2018) 1–11.
[61] M.A. Murcko, Ajay, Computational methods to predict binding free energy in ligand-receptor complexes, J Med Chem. 38 (1995) 4953–4967.
[62] X. Du, Y. Li, Y.-L. Xia, S.-M. Ai, J. Liang, P. Sang, X.-L. Ji, S.-Q. Liu, Insights into protein–ligand interactions: mechanisms, models, and methods, Int J Mol Sci. 17 (2016) 1–34.
[63] A.K. Bronowska, Bronowska, Thermodynamics of Ligand-Protein Interactions: Implications for Molecular Design, Thermodynamics - Interaction Studies - Solids, Liquids and Gases, 2011: pp. 1–48.
[64] Y. Modis, S. Ogata, D. Clements, S.C. Harrison, Structure of the dengue virus envelope protein after membrane fusion, Nature. 427 (2004) 313–319.
[65] E.A. Christian, K.M. Kahle, K. Mattia, B.A. Puffer, J.M. Pfaff, A. Miller, C. Paes, E. Davidson, B.J. Doranz, Atomic-level functional model of dengue virus Envelope protein infectivity, PNAS. 110 (2013) 18662–18667.
[66] A. Mir, H. Ismatullah, S. Rauf, U.H.K. Niazi, Identification of bioflavonoid as fusion inhibitor of dengue virus using molecular docking approach, Informat Med Unlock. 3 (2016) 1–6.
[67] R. Bavi, R. Kumar, L. Choi, K.W. Lee, Exploration of novel inhibitors for bruton's tyrosine kinase by 3D QSAR modeling and molecular dynamics simulation, PLoS One. 11 (2016) 1–6.
[68] P. Bonnet, R.A. Bryce, Molecular dynamics and free energy analysis of neuraminidase–ligand interactions, Protein Sci. 13 (2004) 946–957.
[69] I. Aier, P.K. Varadwaj, U. Raj, Structural insights into conformational stability of both wild-type and mutant EZH2 receptor, Sci Rep. 6 (2016), 34984.
[70] M. Sivaramakrishnan, K. Kandaswamy, S. Natesan, R.D. Devarajan, S.G. Ramakrishnan, R. Kothandan, Molecular docking and dynamics studies on plasmepsin V of malarial parasite Plasmodium vivax, Inform Med Unlock. 19 (2020) 1–7.
[71] C.G. Gadhe, M. Kim, Insights into the binding modes of CC chemokine receptor 4 (CCR4) inhibitors: a combined approach involving homology modelling, docking, and molecular dynamics simulation studies, Mol BioSyst. 11 (2015) 618–634.
[72] N.C. Benson, V. Daggett, Large-scale assessment of native protein flexibility, Protein Sci. 17 (2008) 2038–2050.
[73] Y. Zhao, C. Zeng, M.A. Massiah, Molecular dynamics simulation reveals insights into the mechanism of unfolding by the A130T/V mutations within the MID1 Zinc-Binding Bbox1 domain, PLoS One. 10 (2015) 1–11.
[74] H.T.T. Lai, A. Giorgetti, G. Rossetti, T.T. Nguyen, P. Carloni, A. Kranjc, The interplay of cholesterol and ligand binding in hTSPO from classical molecular dynamics simulations, Molecules. 26 (2021) 1–23.
[75] J. Zhu, Y. Lv, X. Han, D. Xu, W. Han, Understanding the differences of the ligand binding/unbinding pathways between phosphorylated and non-phosphorylated ARH1 using molecular dynamics simulations, Sci Rep. 7 (2017) 1–14.
[76] A. Gutteridge, J. Thornton, Conformational change in substrate binding, catalysis and product release: an open and shut case? FEBS Lett. 567 (2004) 67–73.
[77] M. Tarek, D.J. Tobias, The role of protein-solvent hydrogen bond dynamics in the structural relaxation of a protein in glycerol versus water, Eur Biophys J. 37 (2008) 701–709.
[78] D. Zhang, R. Lazim, Application of conventional molecular dynamics simulation in evaluating the stability of apomyoglobin in urea solution, Sci Rep. 7 (2017) 1–12.
[79] B. Kamaraj, R. Purohit, In Silico Screening and Molecular Dynamics Simulation of Disease-Associated nsSNP in TYRP1 Gene and Its Structural Consequences in OCA3, BioMed Res Int. 2013 (2013) 1–13.
[80] R. Dash, M.C. Ali, N. Dash, M.A.K. Azad, S.M.Z. Hosen, M.A. Hannan, I.S. Moon, Structural and dynamic characterizations highlight the deleterious role of SULT1A1 R213H polymorphism in substrate binding, International J Molec Sci. 20 (2019) 1–22.
[81] P. Sneha, C. George Priya Doss, Chapter seven - molecular dynamics: new frontier in personalized medicine, in: R. Donev (Ed.), Advances in Protein Chemistry and Structural Biology, Academic Press, 2016: 181–224.
[82] P. Nagy, Competing intramolecular vs. intermolecular hydrogen bonds in solution, IJMS. 15 (2014) 19562–19633.
[83] M. Petukhov, G. Rychkov, L. Firsov, L. Serrano, H-bonding in protein hydration revisited, Protein Sci. 13 (2004) 2120–2129.
[84] S.N.H. Ishak, S.N.A.M. Aris, K.B.A. Halim, M.S.M. Ali, T.C. Leow, N.H.A. Kamarudin, M. Masomian, R.N.Z.R.A. Rahman, Molecular dynamic simulation of space and earth-grown crystal structures of thermostable T1 lipase geobacillus zalihae revealed a better structure, Molecules. 22 (2017) 1–13.
[85] I. Chikalov, P. Yao, M. Moshkov, J.-C. Latombe, Learning probabilistic models of hydrogen bond stability from molecular dynamics simulation trajectories, BMC Bioinform. 12 (2011) 1–6.
[86] J.L. England, G. Haran, Role of solvation effects in protein denaturation: from thermodynamics to single molecules and back, Ann Rev Phys Chem. 62 (2011) 257–277.
[87] L. Voit-Ostricki, S. Lovas, C.R. Watts, Conformation and domain movement analysis of human matrix metalloproteinase-2: role of associated Zn2+ and Ca2+ Ions, IJMS. 20 (2019) 1–19.
[88] Y-C. Hsieh, F. Poitevin, M. Delarue, P. Koehl, Comparative normal mode analysis of the dynamics of DENV and ZIKV capsids, Front Mol Biosci. 3 (2016) 1–15.